Analyzing Control Challenges for Thermal Energy Storage in Foodstuffs

Hovgaard, Tobias Gybel; Larsen, Lars F. S. ; Skovrup, Morten Juel; Jørgensen, John Bagterp

Published in:
2012 IEEE International Conference on Control Applications (CCA)

Link to article, DOI:
10.1109/CCA.2012.6402413

Publication date:
2012

Document Version
Publisher's PDF, also known as Version of record

2012 IEEE International Conference on Control Applications (CCA)
Part of 2012 IEEE Multi-Conference on Systems and Control
October 3-5, 2012. Dubrovnik, Croatia

Analyzing Control Challenges for Thermal Energy Storage in Foodstuffs

Tobias Gybel Hovgaard, Lars F. S. Larsen, Morten J. Skovrup, and John Bagterp Jørgensen

***Abstract*— We consider two important challenges that arise when thermal energy is to be stored in foodstuffs. We have previously introduced economic optimizing MPC schemes that both reduce operating costs and offer flexible power consumption in a future Smart Grid. The goal is to utilize the thermal capacity of refrigerated goods in a supermarket to shift the load of the system in time without deteriorating the quality of the foodstuffs. The analyses in this paper go before closing any control loops. In the first part, we introduce and validate a new model with which we can estimate the actual temperatures of refrigerated goods from available air temperature measurements. This is based on data obtained from a dedicated experiment. Since limits are specified for food temperatures, the estimate is essential for full exploitation of the thermal potential. Secondly, the thermal properties, shapes and sizes of different foodstuffs make them behave differently when exposed to changes in air temperature. We present a novel analysis based on Biot and Fourier numbers for the different foodstuffs. This provides a valuable tool for determining how different items can be utilized in load-shifting schemes on different timescales and for estimating maximum energy storage time. The results are shown for a large range of parameters, and with specific calculations for selected foodstuff items.**

NOMENCLATURE

$\dot{Q}$	Energy flow (W)
M	Mass (kg)
$\dot{m}$	Mass flow $(kg\ (dry\ air)/s)$
T	Temperature $(^\circ C)$
ΔT	Temperature difference (K)
P	Pressure (Pa)
Cp	Specific heat capacity $(J/(kg \cdot K))$
UA	Overall heat transfer coefficient (J/K)
l_{sh}	Relative length of superheat zone
I	Enthalpy of humid air $(J/kg\ (dry\ air))$
RH	Relative humidity $(\%)$
x	Absolute humidity $(kg/kg\ (dry\ air))$
h	Enthalpy (J/kg)
Δh_{lg}	Latent heat (J/kg)
λ	Thermal conductivity $(W/(m \cdot K))$
ρ	Density (kg/m^3)
h_{ext}	Surface heat transfer coefficient $(W/(K \cdot m^2))$

Subscripts:

e	Evaporation	c	Condensing
amb	Ambient	air	Dry air
ref	Refrigerant	$infilt$	Infiltration
$sens$	Sensible	lat	Latent
sh	Superheat	$surf$	Surface
ex	Exchanged		

T.G. Hovgaard and L.F.S. Larsen are with Vestas Technology R&D, Hedeager 42, DK-8200 Aarhus N, Denmark {togho, lfsla}@vestas.com

M.J. Skovrup is with IPU Technology Development, Building 403, DK-2800 Kgs. Lyngby, Denmark mjs@ipu.dk

J.B. Jørgensen is with DTU Informatics, Technical University of Denmark, Building 321, DK-2800 Kgs. Lyngby, Denmark jbj@imm.dtu.dk

I. INTRODUCTION

In Denmark, around 4500 supermarkets consume more than 550,000 MWh annually. This corresponds roughly to 2% of the entire electricity consumption in Denmark. The capacity for energy storage in the refrigerated goods is not exploited by the thermostat (hysteresis) control policy used today and a large potential for energy and cost reductions exits. Preliminary investigations have been carried out in [1]–[4]. However, accurate estimation of the temperature behavior and distribution in the refrigerated foodstuffs is needed in order to take such simulation studies closer to the challenges seen in an actual supermarket.

A major challenge when exploiting thermal capacity in refrigerated goods is that the temperature of the goods is not normally measured in a supermarket setting. Only air temperatures at the inlets and outlets of the display case are known. However, quality demands, and therefore also temperature ranges, are specified for the foodstuffs. Since the dynamics of larger food items like milk or ground meat packages are much slower than the dynamics of the surrounding air, a substantial share of the potential in thermal energy storage is lost, if we cannot estimate the actual temperatures of the goods. In this paper, we present a model of the display case that links food temperatures to the measurements available.

Different goals can be achieved by applying, *e.g.*, economic model predictive control (MPC) strategies for shifting the load of supermarket refrigeration systems: Energy consumption can be minimized by shifting loads to periods with lower outdoor temperatures. Equipment can be dimensioned smaller or operated at more efficient levels by reducing peak loads. Expenditure on power can be reduced by utilizing varying electricity prices, and by participation in a Smart Grid, the system can be rewarded for its flexibility while delivering crucial services to a power grid with increasing amounts of fluctuating renewable energy sources. This is further discussed in [2], [3], [5]. As shown in our previous work load shifting strategies can be beneficial on different time scales. Participation in the primary regulating power market is mostly on a 15-minute timescale. Peak avoidance and/or utilization of short term variations in electricity prices might call for load shifts of around 2 hours, while day/night variations of both weather and prices work on a timescale of up to 12 hours. Depending on the timescale, energy storage potential is not directly given by the thermal mass in a

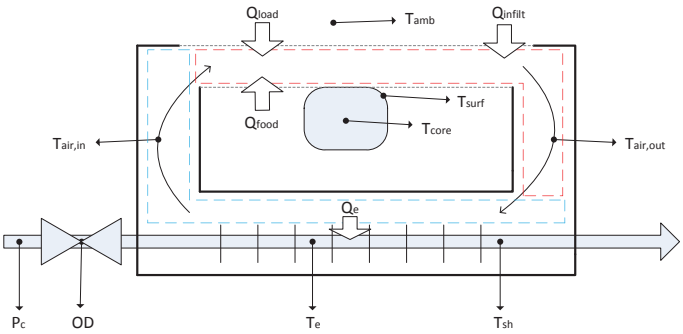

Fig. 1. Refrigerated display case with indications of energy flows, measurements and defined control volumes for air temperatures.

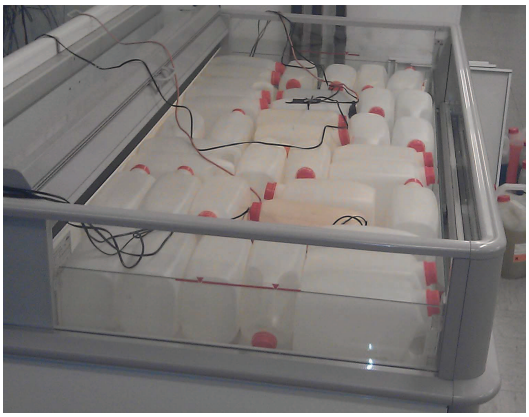

Fig. 2. The experiment setup in the lab.

refrigerated display case. Since only fractions of the stored mass might be affected by the changes in temperature, we introduce the term "active thermal mass". The relevance of applying load shifting strategies on the aforementioned timescales depends on the active thermal mass for a specific item. We analyze this for different types of foodstuffs.

II. SYSTEM DESCRIPTION

The system is a refrigerated display case with a horizontal opening at the top. It is depicted in Fig. 1. Foodstuffs are stacked inside the case where it is kept refrigerated by a "curtain" of cold air flowing between inlets and outlets on either side of the display case. The foodstuffs are hereby separated from the surroundings, and since we disregard any heat transfer by radiation from e.g. light sources in the room, we can assume that heat transfer to/from the foodstuffs only occurs to/from the air curtain. A heat load from the surroundings affects the air curtain both by simple conduction and by infiltration of a degree of ambient air which unavoidably gets mixed into the air stream. The air is circulated by a fan from the air curtain, through a heat exchanger (evaporator) underneath the storage room, and back to the air curtain. In the heat exchanger, heat is removed from the air by evaporation of a refrigerant. The evaporation temperature (T_e) and the opening degree (OD) of an expansion valve at the inlet can be controlled. The superheat temperature is a measure of the distance from the liquid/vapor front to the end of the evaporator, and often an inner loop for superheat control is established. Hence, the set-point of the superheat controller can be considered as a control input instead of the opening degree of the valve.

A. Data set

The data set was collected in the refrigeration lab at Danfoss A/S, Denmark, from a setup using a horizontal 2.5x1.5m supermarket display case. The measured variables (indicated on Fig. 1) are those normally measured in a real supermarket setting; $T_{air,in}$, $T_{air,out}$, T_e, ΔT_{sh}, T_{amb}, OD, and P_c with the addition of two sensors for temperature of the goods; T_{surf} and T_{core}, surface and core temperatures respectively. Canisters filled with ethylenglycol were used to simulate goods instead of actual foodstuffs. A picture of the setup is seen in Fig. 2. As is the case in most supermarkets, temperature control was done by hysteresis using the temperature of the air flow out of the display case with defined upper and lower limits. Since no foodstuffs could be damaged in this experiment, more variation in the temperature than what is normally possible in a supermarket was allowed. The data were sampled every $T_s = 5$ seconds (which is relatively fast compared to the slow dynamics of the system) and pre-processed with a moving average, low-pass filter. According to the specifications of the sensors, the measurements can have a constant offset of up to $0.5K$.

B. Assumptions

In order to formulate the equations in the next section we need to make some assumptions.

- We define two control volumes for the areas surrounding the measured air temperatures. These areas are shown with blue and red dotted lines on Fig. 1. Within each of these volumes, we assume uniform temperatures.
- We scale the cooling energy in the evaporator according to manufacturer's knowledge of maximal capacity. In this case: $\dot{Q}_{e,max} \approx 0.7kW/m \cdot 1.8m = 1260W$.
- According to [6] the load on a horizontal display case without covers is typically divided so that 75% is due to infiltration of ambient air while the remaining 25% (neglecting radiation) is due to conduction. We adopt this ratio here.
- It is assumed that the relative humidity in the lab environment remains constant at 50%. Furthermore, we assume that the relative humidity is approximately 95% in the air flow after the evaporator since the saturation temperature is normally reached such that water is condensed from the air.
- The inner control loop is much faster than the dynamics we are trying to estimate. Thus, it is neglected in the model of the system.

C. Model

Before we apply a grey-box identification technique, the differential equations governing the system dynamics are established. We have chosen four states, namely $T_{air,in}$, $T_{air,out}$,

T_{surf} and T_{core}, and by setting up the energy balances we get (1)-(4).

$$M_{air,1}Cp_{air}\frac{dT_{air,in}}{dt} = \dot{m}_{air}\cdot(I(T_{air,out},RH_{out})- I(T_{air,in},95\%)) - \dot{Q}_{sens} \quad (1)$$

$$M_{air,2}Cp_{air}\frac{dT_{air,out}}{dt} = \dot{m}_{air}\cdot(I(T_{air,in},95\%)- I(T_{air,out},RH_{out}))+ \dot{Q}_{load}+\dot{Q}_{infilt}+\dot{Q}_{food} \quad (2)$$

$$M_{surf}Cp_{food}\frac{dT_{surf}}{dt} = \dot{Q}_{surf-core}-\dot{Q}_{food} \quad (3)$$

$$M_{core}Cp_{food}\frac{dT_{core}}{dt} = -\dot{Q}_{surf-core} \quad (4)$$

Some of the energy flows are given by Newton's law of convection:

$$\dot{Q}_{load} = UA_{amb}\cdot(T_{amb}-T_{air,out}) \quad (5)$$

$$\dot{Q}_{food} = UA_{food}\cdot\left(T_{surf}-T_{air,out}\right) \quad (6)$$

$$\dot{Q}_{surf-core} = UA_{surf-core}\cdot\left(T_{core}-T_{surf}\right) \quad (7)$$

The energy contribution due to infiltration is given by:

$$\dot{Q}_{infilt} = \dot{m}_{ex}\cdot(I(T_{amb},50\%)-I(T_{air,out},95\%)) \quad (8)$$

For the cooling capacity from the evaporator we have chosen the ε-NTU method which is generally accepted for heat exchanger modeling [7]. Here we assume that the method adopts to humid air.

$$\dot{Q}_e = \dot{Q}_{sens}+\dot{Q}_{lat} = \dot{m}_{air}\left(I(T_{air,out},RH_{out})-I(T_e,100\%)\right)\cdot\varepsilon \quad (9)$$

$$\varepsilon = 1-\exp(-NTU) \quad (10)$$

$$NTU = \frac{UA_{evap}\cdot(1-l_{SH})}{\dot{m}_{air}Cp_{air}} \quad (11)$$

where $\dot{Q}_{sens}$ is the amount of energy that goes to cooling the air flow, while the energy used for condensing water out of the air is given by:

$$\dot{Q}_{lat} = \dot{m}_{air}\cdot(x_{air,out}-x_{air,in})\cdot\Delta h_{lg} \quad (12)$$

$$x_{air,out} = x_{air,in}+\frac{\dot{m}_{ex}}{\dot{m}_{air}}\cdot(x_{amb}-x_{air,in}) \quad (13)$$

For calculating the relative length of the superheat zone, we adopt the following equations from [8]:

$$l_{SH} = -\ln\left(1-\frac{T_{SH}}{T_{air,out}-T_e}\right)\frac{\dot{m}_{ref}Cp_{ref}}{UA_{SH}} \quad (14)$$

$$\dot{m}_{ref} = \dot{m}_{air}\frac{I(T_{air,out},RH_{out})-I(T_{air,in},95\%)}{h_{out}-h_{in}} \quad (15)$$

$$h_{out} = HTP(T_{ref,out},T_e),\quad h_{in} = HBub(P_c)$$

where the functions HTP and $HBub$ are nonlinear, refrigerant dependent functions that can be calculated using e.g. the software RefEqns [9]. Additional equations for calculating relative and absolute humidity and enthalpy of humid air are given in [10].

D. Parameters

For the system identification problem based on the equations described in the previous sections, the following parameters are included.
Measured inputs: $T_{sh},\ T_e,\ T_{amb},\ P_c$.
Measured outputs: $T_{air,in},\ T_{air,out},\ T_{surf},\ T_{core}$.
Assumed known: $\dot{m}_{air},\ Cp_{air},\ Cp_{food},\ Cp_{ref}$.
where $\dot{m}_{air}$ is derived from knowledge of the maximum evaporator capacity, as will be shown later.
To be estimated:

$$UA_{SH},\ UA_{evap},\ UA_{amb},\ UA_{food},\ UA_{surf-core},\ M_{air,1},\ M_{air2},\ M_{surf},\ M_{core},\ \dot{m}_{ex},\ offset_1\ \ offset_2\ \ offset_3$$

where UA_{amb} and $\dot{m}_{ex}$ only can be estimated uniquely if the relationship between $\dot{Q}_{load}$ and $\dot{Q}_{infilt}$ is known. The three offsets are used to correct for constant errors in the sensors.

III. SYSTEM IDENTIFICATION

We identify the unknown variables in order to determine the relationship between input/output variables and the food temperatures. The estimation is done in steps for sub-parts of the entire system in order to simplify the calculations and to ensure identifiability.

First, the subsystem consisting of (1)-(2) and the relevant energy equations is considered. This system has the outputs/states $\{T_{air,in},T_{air,out}\}$ and the inputs $\{T_{sh},T_e,T_{amb},P_c,T_{surf}\}$. We use the assumption of maximum cooling capacity and (9) to estimate the mass flow of air circulating in the display case. This results in $\dot{m}_{air} = 0.175kg/s$. The cooling capacity $\dot{Q}_e$ is a non-linear function, so we take a non-linear approach using `idnlgrey` from the System Identification Toolbox in Matlab [11]. Regarding UA_{amb} and $\dot{m}_{ex}$ we fix e.g. $UA_{amb} = 1$ initially. Then we get an estimate of $\dot{m}_{ex}$ and, with the knowledge about the relationship between $\dot{Q}_{load}$ and $\dot{Q}_{infilt}$, a new guess on UA_{amb} is found. By repeating this a couple of times, values with a good fit and with the correct ratio can be estimated. Next, the system with T_{surf} as the only output/state and the inputs $T_{air,2}$ and T_{core} is estimated in the same manner keeping the already identified parameters fixed. The remaining parameters are found from the system with T_{core} as the only output/state and with T_{surf} as input. The resulting parameters are given in Table I.

In e.g. [12], a finite volume method like the one used for the analysis in section IV is compared to a foodstuff model with only a core and surface layer, and it is found that only a small error occurs for most ranges of the parameters.

A. Analysis and Validation

The parameters are validated qualitatively, and a few observations are easily made. All the estimated offsets are within the $0.5K$ tolerance range specified for the sensors. The masses of surface and core parts of the goods correspond to 40 and 122 liters respectively, which seem realistic for our experiment. The mass of air in the display case ($T_{air,2}$) is,

TABLE I

IDENTIFIED PARAMETERS

$\dot{m}_{air}$	0.175	kg/s
Cp_{air}	1012	$J/(kg \cdot K)$
Cp_{food}	2200	$J/(kg \cdot K)$
Cp_{ref}	1348	$J/(kg \cdot K)$
UA_{SH}	2.94	J/K
UA_{evap}	93.66	J/K
UA_{amb}	10.48	J/K
UA_{food}	14.45	J/K
$UA_{surf-core}$	206.34	J/K
$M_{air,1}$	2.18	kg
$M_{air,2}$	66.10	kg
M_{surf}	45.33	kg
M_{core}	136	kg
$\dot{m}_{ex}$	0.0023	kg/s
$offset_1$	-0.29	K
$offset_2$	0.35	K
$offset_3$	0.14	K

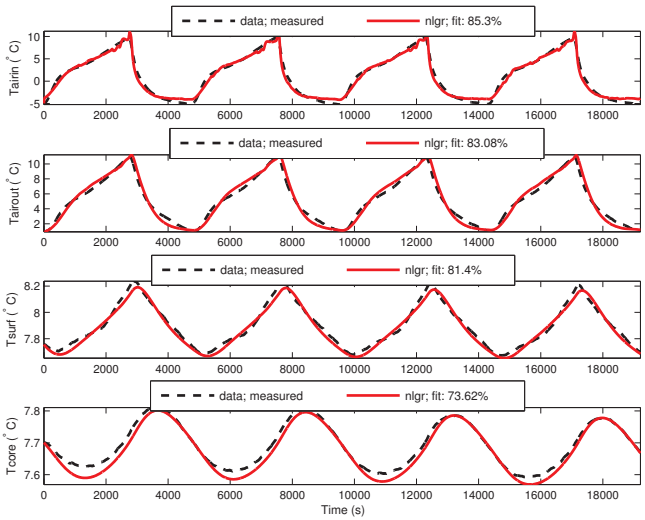

Fig. 3. Comparison of simulated data versus measured data for the test data set. Duration is approximately 5.3 hours.

however, much larger than what can possibly be contained in the display case. But we are aware of several unmodeled effects such as heat capacities in the metal walls. By not including these effects explicitly in the model, the mass of air must account for them, and since the heat capacity and density of metal are much larger than those of air, rather large amounts of air are needed to compensate. The amount of air exchanged with the surroundings is a little less than 2% of the circulated mass flow which also seems reasonable. The sum of the delivered cooling capacity can be compared to the sum of conduction load, infiltration load and exchanged energy with the goods. For the training set, this ratio is 0.96, which is reasonably close to 1.

Fig. 3 shows the identified model versus a validation data set, and it is noted that the identified model captures the dynamics of the system quite well.

IV. ENERGY POTENTIAL IN FOODSTUFFS

We investigate the temperature distribution inside the refrigerated foodstuff by assuming that the foodstuff in question can be compared to a ball that is divided into a finite number of shells. For each shell, the energy balance is formulated by (16)-(18) following the procedure in [12]. $n \in \{1,2,\ldots,N\}$ is the shell number from the center and out, and R is the radius of the ball. The inner shell is shaped like a ball. Hence, for $n = 1$:

$$\rho \cdot V_1 \cdot Cp \cdot \frac{dT_1}{dt} = \frac{\lambda}{\Delta r} \cdot A_1 \cdot (T_2 - T_1) \tag{16}$$
$$V_1 = \frac{4}{3}\pi \cdot \Delta r^3, \quad A_1 = 4\pi \cdot \Delta r^2, \quad \Delta r = \frac{R}{N}$$

For $n \in \{2,\ldots,N-1\}$, the shell is shaped like a sphere for which:

$$\rho \cdot V_n \cdot Cp \cdot \frac{dT_n}{dt} = \frac{\lambda}{\Delta r}(A_{n-1} \cdot (T_{n-1} - T_n) + A_n \cdot (T_{n+1} - T_n)) \tag{17}$$
$$V_n = \frac{4}{3}\pi \cdot \left(\left(\frac{n \cdot R}{N}\right)^3 - \left(\frac{(n-1) \cdot R}{N}\right)^3\right), \; A_n = 4\pi \cdot \left(\frac{n \cdot R}{N}\right)^2$$

For the outer shell, the boundary condition to the surrounding air applies. Hence:

$$\rho \cdot V_N \cdot Cp \cdot \frac{dT_N}{dt} = \frac{\lambda}{\Delta r} \cdot A_{N-1} \cdot (T_{N-1} - T_N) - h_{ext} \cdot A_N \cdot (T_{surf} - T_{air}) \tag{18}$$
$$T_{surf} = \frac{\frac{\lambda}{0.5 \cdot \Delta r} \cdot T_N + h_{ext} \cdot T_{amb}}{\frac{\lambda}{0.5 \cdot \Delta r} + h_{ext}}$$

Eq. (16)-(18) leads to a dynamic state for each shell in the model. It was found that 10 layers are sufficient for the average size of foodstuff. In addition, we added an extra state, E, integrating the heat flux in and out of the surface layer. By simple frequency analysis of this linear model (from T_{air} to E), it is seen how much energy that can be stored in the specific foodstuff at a specific frequency. We found that the response is very similar to a first order system with a flat DC-gain up to a certain cut-off frequency where it declines for increasing frequencies, until it flattens out at zero gain for very high frequencies. Interpreting this in the context of a layered food model, the DC-gain is the energy stored in an item when its entire mass has taken on the same temperature as the surrounding air, per Kelvin change in air temperature. For higher frequencies, the air temperature changes faster than the inner shell temperature can follow, and the temperature of the item is a function of depth from the surface. Thus, only a fraction of the item's mass is activated for energy storage.

The load-shifting potential is also limited from below on the frequency scale. Even though the entire mass is activated there is a limit to how long the temperature of the outer shell will remain below its upper limit. Therefore, it does not make sense to use the DC-gain as an indicator of the potential on very long timescales. The stored energy will simply disappear from the food item before the time it was

stored for. Using the system from (16)-(18), we can set up the model from T_{air} to T_N (the outer layer that will violate the upper temperature limit first). The 99% rise time of a step response for this system is then used as the upper limit for the time we are able to shift the load for a particular item.

For calculations on a selection of different foodstuffs we have used thermal properties from the data and studies in [13]–[15]. The investigated foodstuffs are: 1-L cow's milk, 500-g of ground beef both refrigerated and frozen, 1-kg frozen solid meat, 50-g of sliced ham, 1-kg frozen vegetables, 2-L fruit juice, a frozen chicken, a fresh egg and 100-L milk tightly packed in a rack.

The solutions to energy storage potential and maximum storage time can be uniquely described by two numbers, the Biot (Bi) number (the ratio of the heat transfer resistances inside and at the surface of a body) and the Fourier (Fo) number (the ratio of the heat conduction rate to the rate of thermal energy storage). These are defined as:

$$Bi = \frac{h \cdot R}{\lambda} \tag{19}$$

$$Fo = \frac{\lambda \cdot t}{\rho \cdot Cp \cdot R^2} \tag{20}$$

In (20) and onwards t is used for the characteristic time which we here use as the load-shifting time, or the time from minimum to peak (half a period) for a sinusoid.

A. Results

By sweeping reasonable ranges for the thermal properties, item sizes and characteristic times, the frequency and rise time analyses mentioned are performed for a range of Biot-Fourier combinations. The energy storage potential for each combination of parameters is found by selecting the magnitude corresponding to the frequency $\omega = \frac{1}{2 \cdot t} 2\pi rad/s$, where t is the characteristic time. The result is normalized by maximum potential ($\rho \cdot Cp \cdot V$) to get a value between 0 and 1. The rise time is calculated from a step response for each combination of parameters and multiplied by Fo/t in order to be converted to a Fourier number. The result is given in Fig. 4 where the contours are active thermal mass as a fraction of total available thermal mass per degree temperature change in the surrounding air. We also indicate the maximum time period for energy storage in the figure.

In Fig. 4 the locations of the 10 different types of foodstuffs are shown by dotted horizontal lines. For each of the chosen items the Biot number is constant, whereas the Fourier number depends on the time.

For each food item and for each of the three timescales the energy storage potential (ESP) is found by reading the active thermal mass ratio from the plot and multiplying by total energy potential ($\rho \cdot Cp \cdot V$) for that item. The results are shown in Table II sorted by Biot number. The rise times for the outer shell are given in hours in the table. From the results in table II we observe how different foodstuffs are suitable for energy storage on different timescales and how some items, e.g. a frozen chicken, are not suitable for 12-hour load shifting. This might be a surprising result. Frozen vegetables and fresh eggs can utilize quite large portions of their potential on the two shortest timescales, while milk, fruit juice and refrigerated ground beef seem to be better suited for energy storage on longer timescales. In this study milk is the only item we have considered as both a single item and as a tightly packed number of items. This, of course, can be done for all other types of foodstuffs that are normally packed in a display case by changing the size appropriately. As seen for milk. this drastically extends the period for which the potential can be utilized; however, on the other hand, it severely decreases the fraction of total potential on the shorter timescales.

B. Other Considerations

A few additional factors other than those analyzed in this paper will affect the energy storage potential that can be utilized in load-shifting strategies. One such factor is the duty cycle of the respective display case inlet valve. If the heat load on the display case is almost equal to the maximum available cooling capacity, the average on-time will be high, meaning that there is only a limited freedom for load shifting regardless of the potential in the goods. As the results in the previous section are calculated per mass unit and per degree change in air temperature, the actual potential greatly depends on both the amount of the foodstuff normally kept in a display case, how it is packed and the specific range of allowable temperatures for preserving the food quality. Finally, the rise time as indicator of maximum storage time used in this paper is only valid if the air temperature is changed to the upper limit of allowable temperatures. If, instead, it is changed to the temperature of the surroundings, the rise time should be calculated as a smaller fraction of the step size.

V. CONCLUSIONS

We have established an important relationship between measured variables in a supermarket refrigeration system and the food temperatures that are in play when applying thermal energy storage strategies. This enables a higher degree of utilization of storage potential. In addition, we investigated the thermal properties of different foodstuffs and the link to their temperature distributions. Thereby, we introduced the "active thermal mass", which is an important measure of energy storage potential. Our analysis linked the Biot and Fourier numbers of food items to both "active thermal mass" and maximum energy storage time. The main findings in Fig. 4 show how most food items are appropriate for time shifting within 2 hours, and that a few food items can be used for almost 12-hour load shifts.

ACKNOWLEDGMENT

The authors gratefully thank Danfoss Electronic Controls R&D, Refrigeration and Air-conditioning, Nordborgvej 81, DK-6430 Nordborg, Denmark for their contributions and support.

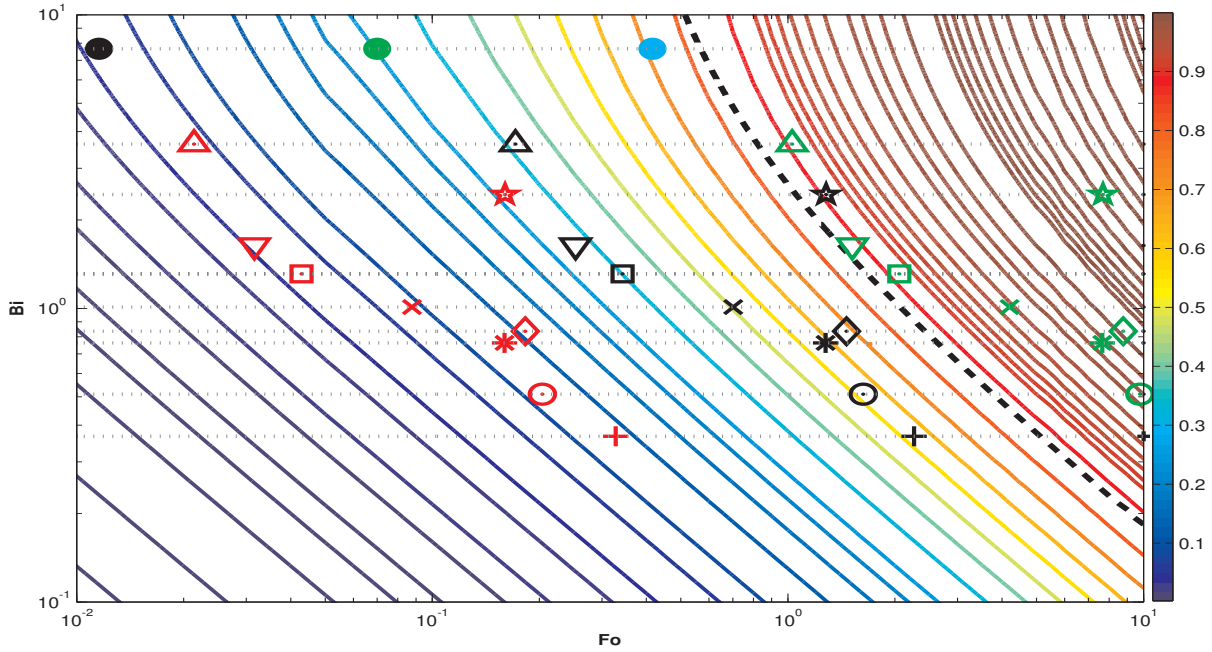

Fig. 4. Energy storage potential versus Biot and Fourier numbers in a double logarithmic scale. The dashed black line indicates the 99% rise time as a Fourier number. Symbols show where different foodstuffs are located in the space as a function of time. Red = 15 min, black = 2 hours, green = 12 hours and cyan = 72 hours. Each horizontal dotted line indicates a selected food item. Refer to Table II, where the types of foodstuffs are shown with their symbols.

TABLE II

ENERGY STORAGE POTENTIAL FOR DIFFERENT FOODSTUFFS, SORTED BY BIOT NUMBER, AT DIFFERENT TIMESCALES. ENERGIES ARE IN J/K.

Symbol	Food item	$\rho \cdot Cp \cdot V$	ESP, 15 min	ESP, 2 hours	ESP, 12 hours	Rise time (h)
+	50-g ham	121	11	75	NA	3.8
○	500-g ground beef, frozen	850	76	486	NA	4.5
∗	1-kg solid meat, frozen	1,729	167	1,034	NA	4.1
♢	Fresh egg	183	25	128	NA	3.3
×	Whole chicken, frozen	5,928	414	2.881	NA	6.1
□	500-g ground beef	1,569	79	513	1,397	9.9
▽	1-L cow's milk	3,917	157	1,124	3,408	11.1
⋆	1-kg vegetables, frost	1,494	356	1,267	NA	2.3
△	2-L fruit juice	7,710	463	2,544	6,862	9.3
•	100-L milk in rack	400,876	4,009	20,044	88,193	96.9

REFERENCES

[1] L. F. S. Larsen, C. Thybo, and H. Rasmussen, "Potential energy savings optimizing the daily operation of refrigeration systems," *Proc. European Control Conference, Kos, Greece*, pp. 4759–4764., 2007.

[2] T. G. Hovgaard, L. F. S. Larsen, and J. B. Jørgensen, "Flexible and Cost Efficient Power Consumption using Economic MPC - A Supermarket Refrigeration Benchmark," in *IEEE Conference on Decision and Control and European Control Conference*, 2011, pp. 848–854.

[3] T. G. Hovgaard, L. F. Larsen, K. Edlund, and J. B. Jørgensen, "Model predictive control technologies for efficient and flexible power consumption in refrigeration systems," *Energy*, 2012.

[4] T. G. Hovgaard, L. F. S. Larsen, M. J. Skovrup, and J. B. Jørgensen, "Optimal energy consumption in refrigeration systems - modelling and non-convex optimisation," *The Canadian Journal of Chemical Engineering*, p. in press, 2012.

[5] T. G. Hovgaard, L. F. S. Larsen, J. B. Jørgensen, and S. Boyd, "Nonconvex model predictive control for commercial refrigeration," http://www.stanford.edu/~boyd/papers/noncvx_mpc_refr.html, 2012.

[6] Y. Ge and S. Tassou, "Performance evaluation and optimal design of supermarket refrigeration systems with supermarket model "supersim", part i: Model description and validation," *International Journal of Refrigeration*, vol. 34, no. 2, pp. 527–539, 2011.

[7] D. P. Dewitt, F. P. Incropera, and T. L. Bergman, *Fundamentals of heat and mass transfer*. John Wiley & Sons, New York, 1996.

[8] H. Rasmussen and L. F. S. Larsen, "Nonlinear superheat and capacity control of a refrigeration plant," *2009 17th Mediterranean Conference on Control and Automation*, pp. 1072–1077, 2009.

[9] M. Skovrup, "Thermodynamic and thermophysical properties of refrigerants - software package in borland delphi." Department of Energy Engineering, Technical University of Denmark, Tech. Rep., 2000.

[10] P. O. Danig and H. V. Holm, "Humid air." Department of Energy Engineering, Technical University of Denmark, Tech. Rep., 1998.

[11] L. Ljung, *System Identification - Theory for the User*, 2nd ed. Prentice Hall, 1999.

[12] R. van der Sman, "Simple model for estimating heat and mass transfer in regular-shaped foods," *Journal of Food Engineering*, vol. 60, no. 4, pp. 383–390, 2003.

[13] Y. A. Çengel and A. J. Ghajar, *Heat and Mass Transfer: Fundamentals and Applications*. McGraw-Hill, 2010.

[14] A. G. Fikiin, K. A. Fikiin, and S. D. Triphonov, "Equivalent thermophysical properties and surface heat transfer coefficient of fruit layers in trays during cooling," *Journal of Food Engineering*, vol. 40, no. 1-2, pp. 7 – 13, 1999.

[15] I. Dincer and O. F. Genceli, "Cooling of spherical products: Part iiheat transfer parameters," *International Journal of Energy Research*, vol. 19, no. 3, pp. 219–225, 1995.